Physica Scripta. Vol. T5, 178–182, 1983.

High Spin Phenomena in the Mass 100–200 Region Seen Through the Crystal Ball

J. J. Gaardhøje, J. D. Garrett, G. B. Hagemann, B. Herskind, A. Holm, P. Nolan* and G. Sletten

The Niels Bohr Institute, University of Copenhagen

J. R. Beene, M. L. Halbert, D. C. Hensley, I. Y. Lee and F. Plasil

HHIRF, Oak Ridge National Laboratory, Oak Ridge, Tennessee

F. A. Dilmanian, M. Jääskeläinen,† H. Puchta, D. G. Sarantites and R. Woodward

Washington University, St. Louis, Missouri

and

Th. Lindblad

Research Institute of Physics, Stockholm

Received October 26, 1982; accepted December 10, 1982

Abstract

The average properties of the gamma ray entry region and the decay from it are studied systematically, for 49 nuclear systems, in the spin spectrometer. Preliminary results are given for the mass the neutron number dependence of the gamma ray fold distribution and of unresolved γ spectra. The possibility of gating simultaneously on narrow regions of fold and excitation energy is exploited.

1. Introduction

The development of high spin gamma ray spectroscopy has in the past ten years been characterized by the use of ever more complex detection systems, aimed at collecting a large fraction of the gamma rays emitted by nuclei produced at high rotational energies and angular momenta. The total gamma ray energy has been collected with efficiencies of 60–90% with the use of sum spectrometers [1], while the moments of the γ-ray multiplicity distributions have been measured in arrays consisting of typically 10–15 small NaI(Tl) detectors [2, 3]. The advantages of both techniques are combined in a new type of instrument, the Spin Spectrometer, popularly known as the Crystal Ball, which features a solid angle close to 4π and a good multiplicity resolution due to the large number of detectors employed. This type of detector system permits the collection of high quality nuclear structure information in coincidence with high resolution γ-ray and particle detectors at an unprecedented data rate.

This contribution reports on a survey experiment done with the Spin Spectrometer operating at the Holifield Heavy Ion facility at Oak Ridge National Laboratory and presents some of the preliminary results. The purpose of the experiment has been to study the average properties of the gamma decay for a large number of nuclear systems (A = 100–200) in a series of short ($\simeq$ 2 h) runs on each target. Apart from obtaining new systematic information on the bulk properties of nuclear structure at extreme spins it is hoped that this survey will outline new and interesting regions of the isotope chart for future more detailed studies.

2. Experimental conditions

The ORNL Spin Spectrometer, its performance and its calibration have been described in detail by Jääskeläinen et al. [4].

In the present experiment the spectrometer was triggered by any of the following detectors. A Ge(Li)-detector located at 117° with respect to the beam direction, two external (5″ x 6″) NaI(Tl)-detectors located 90 cm from the target at angles 0° and 87°, three (E, dE/dx)-particle telescopes kept at 40°, 90° and 140° in the center of mass frame and two surface barrier detectors located at $\simeq \pm 7°$, intended for collecting the fused recoiling nuclei. In addition, two solid state fission detectors were used and located symmetrically at the mean fission opening angle which varies according to the kinematics of the reaction. The solid angles were adjusted to ensure a balanced trigger rate among the various detectors.

For each event the energy and time signals were recorded for the trigger detectors and the 68 NaI detectors of the spectrometer, subject to the condition that the total gamma ray fold be $\geqslant 4$ for events triggered by a gamma detector and $\geqslant 2$ for events triggered by one of the particle detectors. From this information the total gamma ray fold, k, and pulse height, H, can be evaluated.

A total of 49 targets were irradiated with a ^{50}Ti beam forming systems with masses from $A = 95$ to $A = 204$. Whenever possible, series of isotopes were produced. The targets were 1–3 mg/cm^2 thick and in most cases self supported. The beam energy was kept fixed at 230 MeV, i.e., sufficiently high to exceed the fission barrier predicted by the liquid drop model [5] for most of the studied systems. This is possible, since the large energy associated with the center of mass motion in the lighter systems, is to a large extent compensated by the lower coulomb barrier.

---

* Permanent address: Oliver Lodge Laboratory, University of Liverpool, England.

† Present address: Department of Physics, University of Jyväskylä, Jyväskylä, Finland.

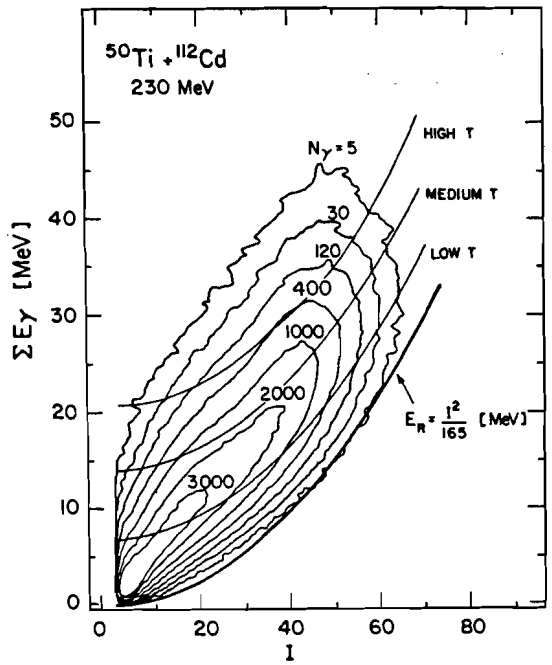

Fig. 1. Total gamma-ray entry state distribution for ^{162}Yb*. The conversion from the experimental quantities H and k to total energy E_γ vs. spin I, is discussed in the text.

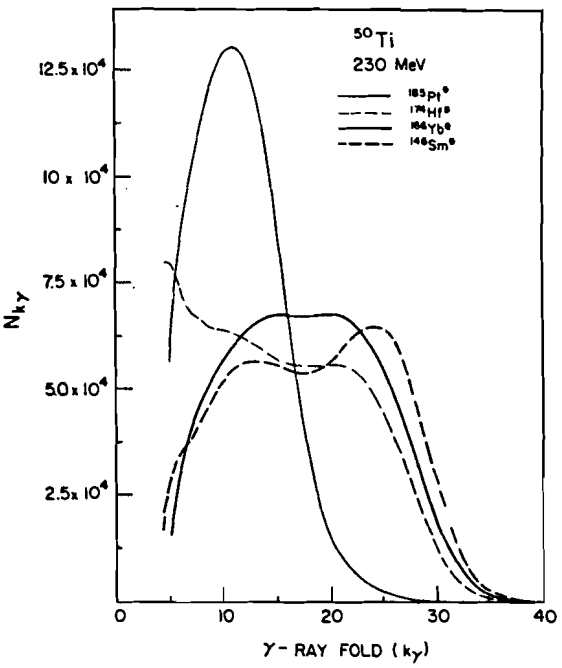

Fig. 2. Gamma-ray fold (k_γ) distributions as a function of the nuclear mass A. The curves have been normalised to the same number of events. The shapes of the distributions are biased by the larger triggering probability (proportional to k_γ) of the gamma detectors wherefore high multiplicity events related to the compound decay are emphasized.

3. Spin spectrometer data

3.1. *Gamma ray fold distributions*

The gamma ray entry distribution (i.e., the loci of the starting point of gamma ray cascades after particle evaporation) is depicted in Fig. 1 for the ^{166}Yb compound system. The transformation from the measured pulse height (H) vs. fold (k) distribution to the excitation energy (E^*) vs. multiplicity (M) distribution requires a full two-dimensional unfolding using the measured instrumental response. Such a procedure has not yet been applied. For the present discussion, an average correction involving the known total energy efficiency (0.8) has been used. In labelling the spin axis the following relation

$$I = 2k - 3 \qquad (1)$$

has been assumed. The true fold to spin conversion also involves the detailed knowledge of the multipolarity of the emitted radiation. With the spin spectrometer it is now possible, for the first time, to measure the angular distribution of the γ-rays with respect to the direction defined by the spin vector on an event-by-event basis.

It is interesting to note that the lowest contour of the entry distribution agrees well with the rotational energy calculated from

$$E_R = \frac{\hbar^2}{2J} I(I+1) \simeq \frac{\hbar^2}{2J} I^2 \qquad (2)$$

where $\hbar^2/2J = 165\,\mathrm{MeV}^{-1}$ has been used. This indicates, that the entry states extend all the way down to the yrast line, thus making the selection of very cool systems possible. The total width of the entry distribution is $\simeq 25$ MeV while the FWHM is only $\simeq 9$ MeV. It is stressed that no detailed conclusions should be drawn before the effect of scattering and summing of γ-rays in the detectors is removed, although this is not expected to produce major changes.

Figure 2 shows the projected gamma ray fold distribution for the systems ^{146}Sm*, ^{166}Yb*, ^{174}Hf* and ^{185}Pt*. As expected large variations are observed. The highest γ-fold ($k \simeq 30$ at the half maximum of the compound distribution) is observed in the ^{146}Sm* decay while it is apparent that other mechanisms limit the gamma decay of the ^{50}Ti + ^{135}Ba reaction. This is borne out by gating on the particle detectors and decomposing the total k-distribution into the contributions from the decay of fission fragments, quasielastic and deep inelastic events, and He ions as shown in Fig. 3 for ^{164}Yb*. The relative scale is arbitrary since the curves shown are not normalized to the individual solid

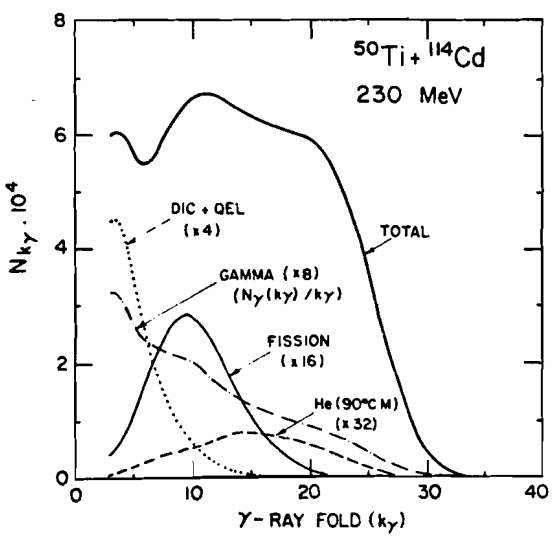

Fig. 3. Total k_γ distributions for the decay of ^{164}Yb*. Also shown is the contribution from the external 0° (5" X 6") NaI(Tl) detector, corrected for the dependence of the triggering probability on the gamma ray fold.

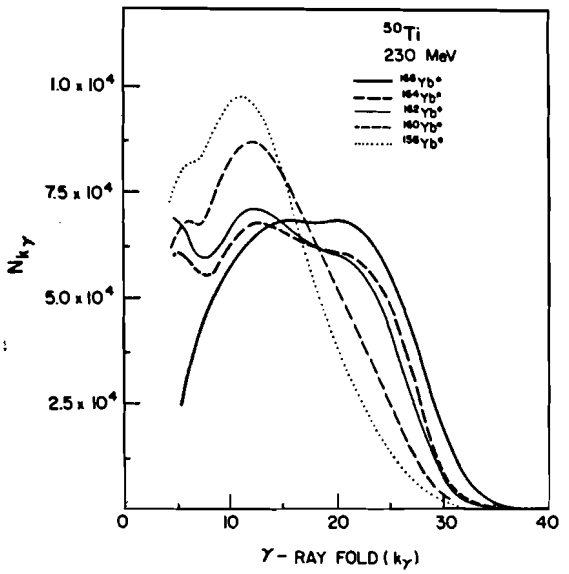

*Fig. 4. Total k_γ distributions for the decay of the Yb isotopes. See the comments in the caption of Fig. 2.

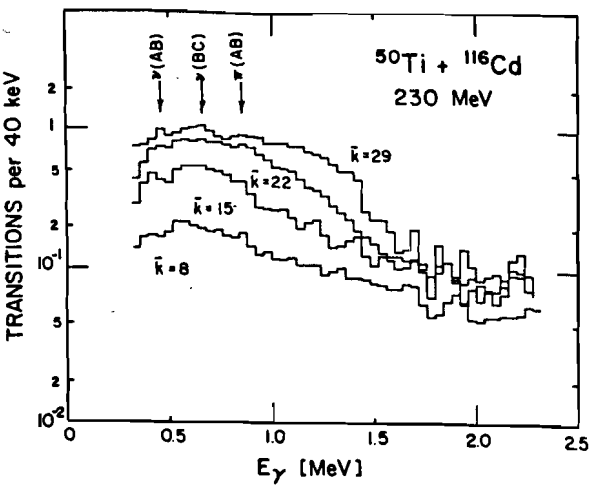

Fig. 5. Unfolded γ-transition energy spectra from the decay of ^{166}Yb gated by four independent fold slices. The spectra recorded at 0° with respect to the beam direction are normalised to the average fold of each of the $\Delta k = 7$ bins. The position of known backbending frequencies in the *xn* products is indicated: ν(AB) = first neutron $(i_{13/2})$bb., ν(BC) = second neutron $(i_{13/2})$bb., and π(AB) = first proton $(h_{11/2})$bb.

angles and efficiencies of the trigger detectors. Indeed, for ^{50}Ti + ^{135}Ba the major component at $k \simeq 11$ is associated with fission events in agreement with the prediction of the rotating liquid drop model (RLDM). Gating on the discrete lines in the Ge(Li) detector reveals the familiar triangular fold distribution expected for the decay of a compound system. Such *xn* fold distributions have been studied by Sarantites et al. [6].

Large variations of the k distributions are also observed in the Yb region as a function of neutron number. In Fig. 4 k_{max} decreases by $\simeq 8$ units from $N = 96$ to $N = 86$, corresponding to an angular momentum reduction of approximately $16\hbar$. The general trend of this reduction is understood from the increase of Γ(fission)/Γ(total) which occurs with decreasing mass (the fissionability varies as Z^2/A). The RLDM predicts that the maximum angular momentum limited by fission should decrease by $8\hbar$ when going from ^{166}Yb* to ^{156}Yb*. Generating the fold distributions in coincidence with α particles results in a similar pattern as a function of N but with k_{max} systematically reduced by $\simeq 3$ units. Since the contribution from α particles to the total k distribution may be important, particularly at the highest spins, this only suggests a lower limit of $\langle \Delta I\hbar \rangle = 6\hbar$ removed by the emitted α particles. No significant variation with α particle energy is observed.

Due to the poorly known discrete spectroscopy in this region it is difficult to estimate the ratio of the α*xn*- to the *xn*-channels in the very light Yb's. For ^{166,164}Yb* the α contribution is however very small, while it becomes more significant in ^{160}Yb*. Since a substantial increase in the cross section for α particle emission is expected in very neutron deficient nuclei [3], part of the observed k reduction may be due to the large removal of angular momentum by α-particles emitted at the highest spins.

3.2. *Continuum gamma ray spectra as a function of angular momentum*

The spin spectrometer offers the possibility of gating selectively on narrow multiplicity intervals and study the coincident transition energy distributions, $E_\gamma(I_k)$, as a function of the angular momentum (I_k) of the entry points.

Figure 5 shows unfolded E_γ spectra from the decay of ^{166}Yb* gated by four independent fold slices corresponding to $\bar{k} = 8$, 15, 22, and 29, respectively. From such spectra it is possible to study the "kinematical" moment of inertia defined by

$$J^{(1)}/\hbar^2 = I\left(\frac{dE_R}{dI^2}\right)^{-1} \simeq \frac{I}{\omega} \tag{3}$$

and which represents the motion of the nuclear system as a body. E_R is to good approximation given by eq. (2). The second derivative of eq. (2) defines the "dynamical" moment of inertia

$$J^{(2)}/\hbar^2 = \left(\frac{d^2E_R}{dI}\right)^{-1} \simeq \frac{dI}{d\omega} \tag{4}$$

which is sensitive to the change of spin with rotational frequency along the decay path. This is the case in the backbending region where a "pile up" of transitions occurs in a narrow frequency interval due to particle alignment. These moments of inertia may be visualised as effective, in the sense that they represent properties of the average decay path followed by the nucleus.

If all transitions are stretched $E2$'s, $dE_R/dI = E_\gamma/2$ and $I = 2N_\gamma$, where N_γ is the number of gamma rays in the cascade. Then,

$$\frac{2J^{(2)}_{eff}}{\hbar^2} = 8\frac{dN_\gamma}{dE_\gamma} \tag{5}$$

which means that in a gamma ray spectrum, the area of which is set equal to the total multiplicity, the height of the spectrum is directly related to $J^{(2)}_{eff}$ if the spectrum is fully populated at all frequencies. A method to correct continuum E_γ spectra for incomplete feeding, has been presented at this conference by M. A. Deleplanque et al.

The main backbending frequencies [7] of the major *xn* products: $4n(^{162}\text{Yb})$, $5n(^{161}\text{Yb})$ and $6n(^{160}\text{Yb})$ are indicated in Fig. 5 and recognised in the higher fold spectra. It is noted that the feeding of the lower k slices is reduced. This may partly be due to events related to reaction products of lower mass, which are important at low multiplicities as may be seen in

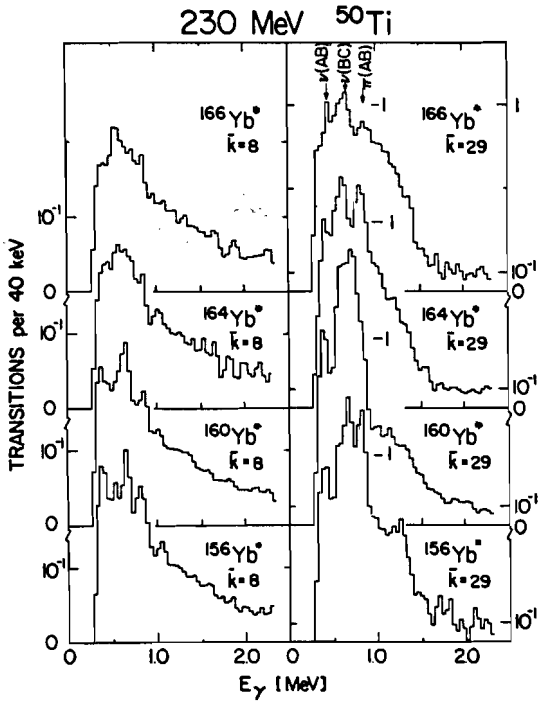

Fig. 6. Unfolded E_γ spectra gated by low and high fold slices ($\Delta K = 7$) for $N = 56$ (^{166}Yb*) through $N = 86$ (^{156}Yb*) recorded in the 0° (5" × 6") NaI(Tl) detector.

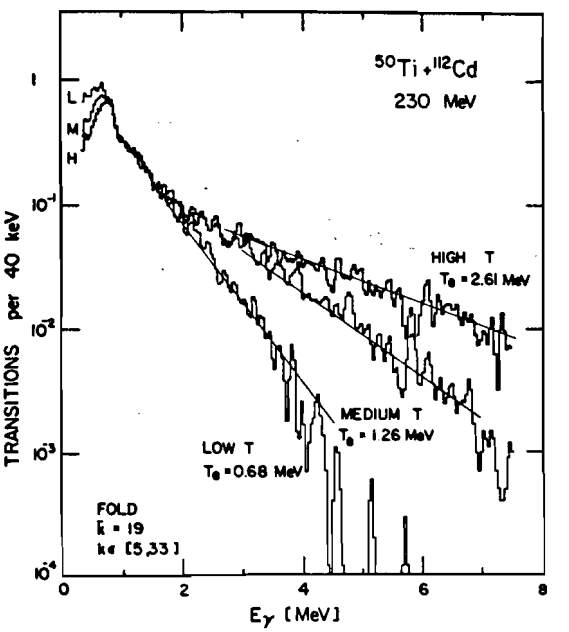

Fig. 7. Unfolded spectra from the decay of ^{162}Yb* gated by the 3 independent temperature regions shown in Fig. 1. The spectra are integrated over all folds in the range $k = 5$–33. The effective temperature T_e corresponding to the statistical part of each spectrum is indicated.

Fig. 3. Indeed the contribution from statistical transitions is roughly expected to be twice as important for fission events as for compound events. Only when selecting narrow k slices at high multiplicities does the low frequency part of the spectra begin to saturate. From the position of the upper edge of the rotational bump one obtains $2\mathcal{J}^{(1)}_{\text{eff}}/\hbar^2 \approx 157\ \text{MeV}^{-1}$ according to eqs. (1) and (3) assuming $\Delta I = 2$ for all transitions.

A comparison between such E_γ spectra gated by low and high folds for four Yb isotopes is shown in Fig. 6. At low k the general shape of the spectra is rather similar consisting of a major bump at $0.3 \lesssim E_\gamma \lesssim 0.9$ MeV. At $\bar{k} = 29$, however, a splitting into two main peaks occurs when moving towards the closed $N = 82$ shell. The lower component is centered at $E_\gamma \simeq 0.7$ MeV. In a contribution to this conference the decay of the final product ^{158}Yb is studied by M. Jääskeläinen et al. A substantial quadrupole content is observed for the lower component at $k \lesssim 20$, while a stretched dipole contribution is reported at higher multiplicities. This is interpreted in terms of a shape change of the nucleus with increasing spin. The measured 0°/90° anisotropies in the present data indicate that the quadrupole content of the lower peak increases at high k with decreasing N. These results agree with studies reported in this conference by F. S. Stephens on the Er isotopes. The higher component which is clearly seen in ^{160,156}Yb* is centered at $E_\gamma \simeq 1.2$ MeV. The motion of its upper edge with multiplicity at high k is consistent with a large quadrupole component. Recent calculations [8] predict the strong alignment of $h_{9/2}[541\ 1/2]$ and $i_{13/2}[660\ 1/2]$ $r = i$ proton orbitals at $\hbar\omega \approx 0.55$ MeV, while a transition to triaxiality is expected at $\hbar\omega \simeq 0.75$ MeV.

3.3. *Temperature selection*

The exciting novel selection technique afforded by the spin spectrometer relies on the simultaneous selection of excitation energy and multiplicity for each individual gamma ray cascade. This allows, for the first time, the identification of decay sequences by the temperature, T, of the region they originate from.

The temperature may be estimated from

$$T = ((E^* - E_R)/a)^{1/2} \tag{6}$$

where a, the level density parameter is, in the harmonic oscillator model, taken to be equal to $A/10$. Figure 7 displays E_γ spectra for ^{162}Yb*, gated by the three isothermal regions indicated in Fig. 1. The most striking effect is evidenced at high E_γ where the logarithmic slopes of the statistical region of the spectra directly reflect the changing effective temperature T_e:

$$\frac{\mathrm{d} \ln N_\gamma}{\mathrm{d}E_\gamma} = -\frac{1}{T_e} \tag{7}$$

The measured T_e values (0.64, 1.26 and 2.61 MeV) may be related to the nuclear temperature T, at each E_γ, by assuming the following energy dependence of the statistical spectrum

$$N_\gamma(E_\gamma) = E_\gamma^{2\lambda+1} S(E_\gamma, \lambda) \exp\left[(E^* - E_R - E_\gamma)/T\right] \tag{8}$$

Here $S(E_\gamma, \lambda)$ represents a gamma ray strength function, constant for $\lambda = 2$, and proportional to E_γ^2 for $\lambda = 1$ as it represents the tail of the giant dipole resonance. This estimate gives

$$\frac{\mathrm{d} \ln N_\gamma}{\mathrm{d}E_\gamma} = \frac{5}{E_\gamma} - \frac{1}{T} \tag{9}$$

independently of the multipolarity and should be compared to eq. (7). The observed T_e corresponds to T_{exp}(low = 0.31 MeV for $E_\gamma = 3$ MeV, T_{exp}(medium) = 0.53 MeV for $E_\gamma = 4.5$ MeV and T_{exp}(high) = 0.82 MeV for $E_\gamma = 6$ MeV. These values may be compared to the estimate obtained from eq. (6) after subtracting the appropriate E_γ from $E^* - E_R$, yielding T_{th}(low) = 0.32 MeV, T_{th}(medium) = 0.56 MeV and T_{th}(high) = 0.79 MeV.

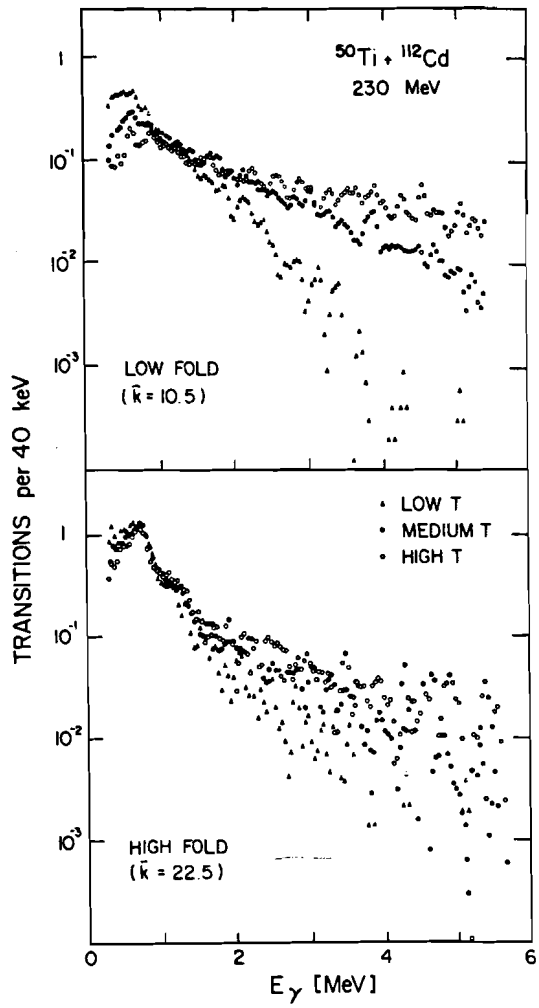

Fig. 8. Unfolded E_γ spectra for $^{162}Yb^*$ gated by the same temperature regions as Fig. 7 but with the additional requirement of low and high fold. The width of each multiplicity bin is $\Delta k = 7$.

This good agreement indicates that the level density parameter used, although not so well founded theoretically, is appropriate for this case. It will be interesting to test whether this is also the case for other systems.

In the region of collective transitions differences are also seen. This is clearly demonstrated in Fig. 8 where similar spectra, with additional multiplicity requirements, are shown. It is noted that the intensity of the high T spectrum is systematically lower at $E_\gamma \lesssim 1$ MeV relative to the lower T spectra, although this difference diminishes in magnitude with increasing k. At low k and high T only few collective transitions remain, and the spectrum shape resembles the one expected for statistical transitions. This is in accordance with the larger contribution of fission related events at low multiplicity which was discussed in the previous section.

At $\bar{k} = 22.5$ a bump at $E_\gamma \simeq 1.2$ MeV, similar to the one in Fig. 6, develops. It is slightly more pronounced in the high T cut. This behaviour is consistent with the interpretation of the high energy bump as due to highly aligned orbits originating from regions of high excitation energy far from the Fermi surface which cross orbitals associated with lower shells. At a given rotational frequency such crossings should be seen first in the high T spectrum.

The decreased feeding observed at low E_γ in the high T and k gated spectra furthermore suggests that immediate cooling down to the yrast line is not dominant (otherwise the spectra should be identical in the collective region), but that the deexcitation at high temperature may proceed along many different paths, which to some extent bypass the yrast region. Such a gradual cooling would result in an average reduction of $J_{eff}^{(2)}$.

More systematic studies of such temperature and multiplicity gated spectra are needed, however, before this important question can be addressed more specifically.

Acknowledgement

This work was supported by the Danish Natural Science Research Council and by NOAC.

References

1. Tjøm, P. O., Espe, I., Hagemann, G. B., Herskind, B. and Hillis, D. L., Phys. Lett. 72B, 439 (1978).
2. Hagemann, G. B., Broda, R., Herskind, B., Ishihara, M., Ogaza, S. and Ryde, H., Nucl. Phys. A245, 166 (1975).
3. Hillis, D. L., Christensen, O., Fernandez, B., Ferguson, A. J., Garrett, J. D., Hagemann, G. B., Herskind, B., Back, B. B. and Folkmann, F., Phys. Lett. 78B, 405 (1978).
4. Jääskeläinen, M., Sarantites, O. G., Woodward, R., Dilmanian, F. A., Hood, J. T., Jääskeläinen, R., Hensley, D. C., Halbert, M. L. and Barker, J. H., Nucl. Instr. Methods (in press).
5. Cohen, S., Plasil, F. and Swiatecki, W., Ann. Phys. 82, 557 (1974).
6. Sarantites, D. G., Jääskeläinen, M., Woodward, R., Dilmanian, F. A., Hensley, D. C., Barker, J. H., Beene, J. R., Halbert, M. L. and Milner, T., Phys. Lett. 115B, 441 (1982).
7. Riedinger, L. L., Andersen, O., Frauendorf, S., Garrett, J. D., Gaardhøje, J. J., Hagemann, G. B., Herskind, B., Makovetzky, Y. V., Waddington, J. G., Guttormsen, M. and Tjøm, P. O., Phys. Rev. Lett. 44, 568 (1980); and Gaardhøje, J. J., Thesis, University of Copenhagen, NBI, (1980).
8. Frauendorf, S., in Proc. of Nobel-Symposium 50, Physica Scripta 24, 349 (1981); and Bengtsson, T. and Ragnarsson, I., Phys. Lett. 115B, 431 (1982).